Degradation of bis-*p*-nitrophenyl phosphate using zero-valent iron nanoparticles

Maiby Valle-Orta[1], David Díaz[2], Inti Zumeta Dubé[2], José Luis Ortiz Quiñonez[2] and Rubén Saldivar Guerrero[1]

[1]Centro de Investigación en Química Aplicada, Blvd. Enrique Reyna Hermosillo No. 140 C.P. 25294 Saltillo, Coahuila/ México and [2]Universidad Nacional Autónoma de México, Facultad de Química, Ciudad Universitaria, Ciudad de México, Coyoacán, C.P.04510/ México.

E-mail: maiby.valle@ciqa.edu.mx

 Abstract. Phosphate esters are employed in some agrochemical formulations and have long life time in the Environment. They are neurotoxic to mammals and it is very difficult to hydrolyze them. It is easy to find papers in the literature dealing with transition metal complexes used in the hydrolysis processes of organophosphorous compounds. However, there are few reports related with degradation of phosphate esters with inorganic nanoparticles. In this work bis-4-nitrophenyl phosphate (BNPP) was used as an agrochemical agent model. The BNPP interaction with zero-valent iron nanoparticles (ZVI NPs), in aqueous media, was searched. The concentration of BNPP was 1000 times higher than the ZVI NPs concentration. The average size of the used iron nanoparticles was 10.2 ± 3.2 nm. The BNPP degradation process was monitored by means of UV-visible method. Initially, the BNPP hydrolysis happens through the P-O bonds breaking-off under the action of the ZVI NPs. Subsequently, the nitro groups were reduced to amine groups. The overall process takes place in 10 minutes. The reaction products were identified employing standard substances in adequate concentrations. The iron by-products were isolated and characterized by X-RD. These iron derivatives were identified as magnetite (Fe_3O_4) and/or maghemite (γ-Fe_2O_3) and lepidocrocite (γ-FeOOH). A suggested BNPP degradation mechanism will be discussed.

1. Introduction

Hydrolysis of phosphoester bonds is involved in many biological processes. They have close relation to information store and conduction, energy transfer and protein phosphoacylation [1]. Phosphoesters have also been the most widely used as pesticides for many decades. They are a large source of potential hazard to humans [2,3]. These compounds are extremely stable and are highly resistant toward hydrolytic processes [4]. Bis-p-nitrophenyl phosphate (BNPP) is a phosphodiester compound that can be used as a model to study the hydrolysis of P-O bonds by catalytic interaction with metal nanoparticles. The stability of this molecule is relatively high; its $t_{1/2}$ is 2000 years in water at 20 °C and 53 years in water at 50 °C [5]. The hydrolytic cleavage of this molecule assisted by transition metal complexes is well-known [6-9]. However, there are few reports related with degradation of phosphate esters with inorganic nanoparticles.

In the other hand, the use of zero-valent iron (ZVI) as reductant to degrade organic contaminant compounds has received considerable attention. Compared with zero-valent iron, ZVI nanoparticles (NPs) have the most promising applications in environmental remediation [10-15]. This effect is due to the decrease of the iron particle size and the increase of the surface area and, thereby, the rate of reaction. The surface area of the ZVI NPs has a direct influence on the number of active surface sites. These sites are called Hot Spots, which are sites for catalytic transformation [16]. The increase of the specific surface area also results in an increase of the fraction of iron atoms that are on the particle surface, thereby, a greater reductive capacity per gram. In other words, these hot spots are places where the electronic hardness is very pronounced (Lewis acid sites or Pearson sites) and they are able to polarize bonds like P-O.

The reductive capacity of the metallic iron is increased when the size of particles is reduced due to the high surface/volume ratio, having greater number of active sites to be carried out this process. Furthermore electron transfer of these nanoparticles is explained by their particle size dependent redox properties.

In this paper, a simple method of BNPP degradation employing ZVI NPs is reported and a mechanism is proposed. In order to reinforce this mechanism, the metallic iron NPs also reacts with standard intermediate products. The degradations were monitored by UV-visible characterization.

2. Materials and Methods

2.1. Materials

Iron(II) bromide, FeBr (98% Aldrich); sodium borohydride, $NaBH_4$, (98% Aldrich); triethylamina, TEA (99.5% Aldrich); ethylene glycol, EG (99.9% J. T. Baker); acetone, $(CH_3)_2CO$, (99.6% J. T. Baker); bis(*p*-nitrophenyl)-phosphate, BNPP (99% Aldrich); *p*-nitrophenol, *p*-NP (99% Aldrich); *p*-nitrophenyl-phosphate, *p*-NPP (99% Aldrich); p-aminophenol, *p*-AP (99% Aldrich); argon, Ar (99.998% Praxair Inc.)

2.2. Instrumentation

High-resolution transmission electron microphotographs (HR-TEM) were obtained in a JEOL 2010 FasTEM analytical microscope, operating at 400 kV, by deposition of a drop of the corresponding dispersion onto 200 mesh copper grids coated with carbon/collodion layers, and processed with Digital Micrograph 1.2 software. The HR-TEM images were used to obtain the particle size distributions. The electronic absorption spectra were collected in a Hewlett-Packard 8452A UV-visible spectrophotometer.

2.3. Synthesis of ZVI NPs

The synthesis of ZV iron NPs in a previous work was published [17] and was carried out as follow: A 0.01078 g portion of $FeBr_2$ was dissolved in 15 mL of ethylene glycol under vigorous stirring and argon bubbling, at room temperature. Then, 0.01890 g of $NaBH_4$ was *in situ* dissolved in 8.75 mL of EG and simultaneously added to the reaction mixture. Instantaneously, a black dispersion of ZVI NPs with gas evolution (molecular hydrogen) was obtained. In order to increase the stability of these NPs, 1.25 mL of 1 M TEA in EG was added to the ZVI dispersion. These stabilized NPs were separated by centrifugation and washed three times with acetone (previously dried in 4 Å zeolites and bubbled with argon for 10 min in order to eliminate the dissolved molecular oxygen). Finally, the resulting black powder was vacuum-dried.

2.4. BNPP degradation studies

The interaction between ZVI NPs and BNPP was carried out as following. 8.65 mg of powder zero-valent iron nanoparticles were suspended in 25 mL of deionized water and argon bubbled, previously. Subsequently, 0.85 mg BNPP were added to this dispersion of nanoparticles under vigorous stirring and allowed to interact for 10 min, the interaction was followed for 1 day. At this

time an aliquot of 8 mL was taken of the reaction mixture, which remains stirring. This portion is centrifuged and the supernatant was taken to measure the UV-visible spectrophotometer. Fe nanoparticles final concentration in this mixture was equal to $1x10^{-7}$ M while the final concentration of BNPP was $1x10^{-4}$ M. Similarly, the interaction between Fe^0 NPs and *p*-nitrophenol (*p*-NP) and *p*-nitrophenyl phosphate (*p*-NPP) were carried out. Afterwards, 0.85 mg BNPP were also added to this dispersion of nanoparticles and allowed to interact for a time range under vigorous stirring.

In order to verify if active iron species were released in the aqueous medium, another experiment was carried out in the same experimental conditions. The zero-valent iron nanoparticles were previously suspended in 25 mL of deionized water and argon bubbled. These nanoparticles were kept under magnetic stirring for 30 minutes. Subsequently, they were centrifuged and separated from the dispersing medium. The volume of total water was used to dissolve 0.85 mg of BNPP and it was kept under stirring for 30 minutes. The electronic absorption spectra were recorded at 10 and 30 minutes.

3. Results

Figure 1 shows a representative ZVI NPs Z-contrast TEM micrograph. The nanoparticles appear agglomerated, forming chain-like structures due to magnetic and electrostatic interactions that exist between them. The average diameter of 10.2 nm (SD ± 3.3 nm) was obtained from 111 counted crystallites from this Z-contrast TEM image.

It is important to mention that the fuzzy appearance of the Z-Contrast image is due to the fact that the magnetic particles are able to deflect the flow of electrons through the observed sample, which results in the presence of astigmatism in the micrograph presented. Other characterizations of ZV iron NPs were published [17].
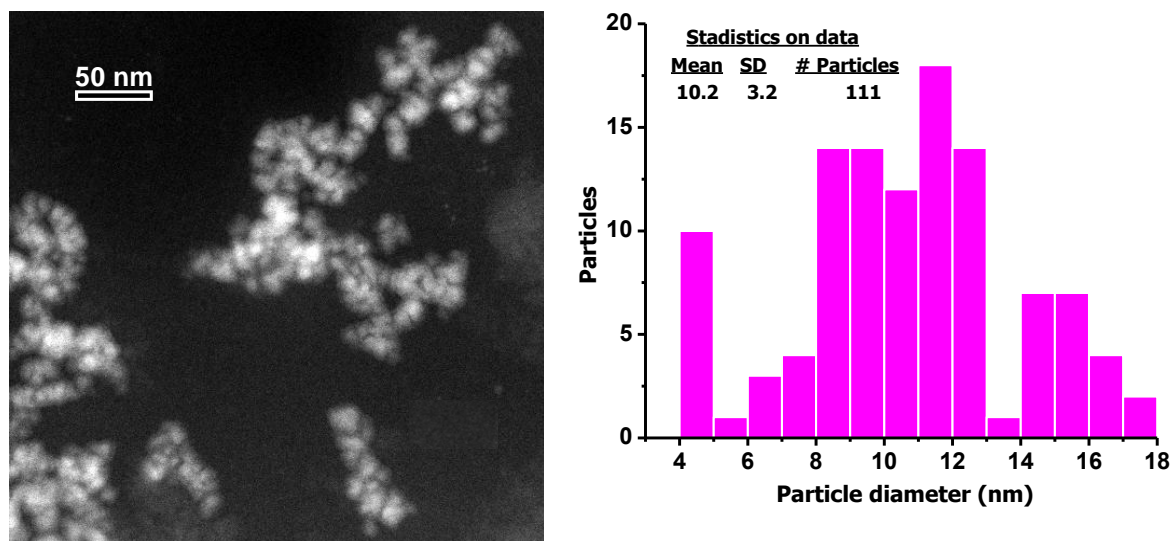

Figure 1. Z-Contrast of ZVI nanocrystallites (after 1 day) prepared from $FeBr_2$ (2×10^{-3} M), $NaBH_4$ (2×10^{-2} M), and TEA (2×10^{-2} M) in ethylene glycol, the corresponding particle size distribution histogram.

Table 1 summarizes the calculated parameters of the ZVI dispersion. These parameters were calculated considering the particle size distribution, assuming a completed reaction (excess of $NaBH_4$ was used) and spherical particles, see reference [17] for details. Parameters in Table 1 correspond to the ZVI NPs obtained in a typical synthesis as described in the Materials and Methods section.

The precursor salt concentration was 2×10^{-3} M. The organic contaminant concentration was calculated considering that BNPP is 1000 times more concentrated than the iron salt concentration for their interaction.

Table 1. Parameters estimated of zero-valent Fe NPs dispersions from data of size distribution.

Metal	Concentration of nanoparticles (particles/mL)	Total surface (m^2)	Relation Surface/volume (m^{-1})
iron	2.04×10^{13}	0.18	5.5×10^8

Figure 2 show the electronic absorption spectra of BNPP during 5 days. As it can be see there was no significant change in band positions during this time. The BNPP provides resistance to natural degradation processes.
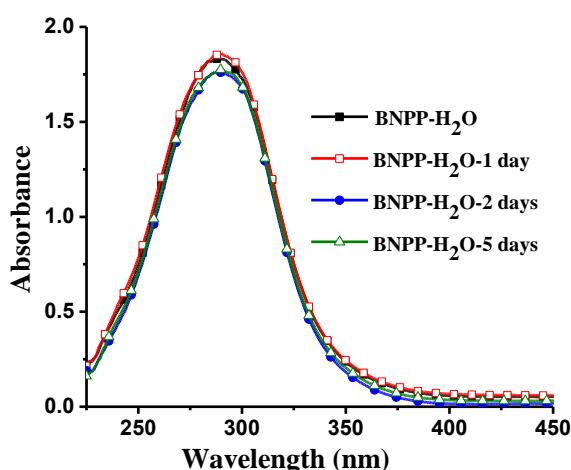

Figure 2. Electronic absorption spectra recorded at room temperature of a BNPP aqueous dissolution (1×10^{-4} M), the final pH was 7.
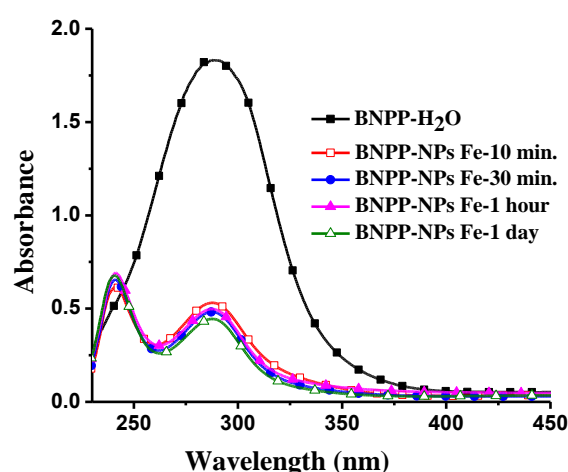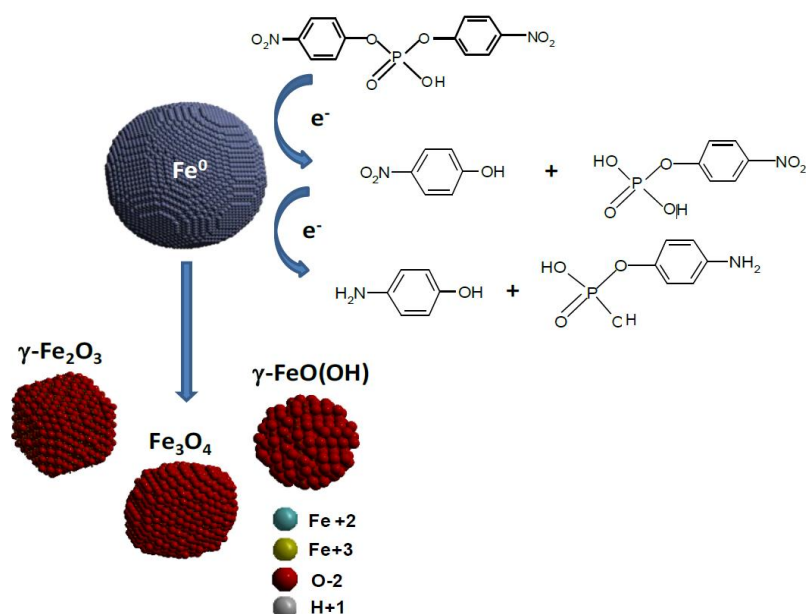
Figure 3. Time-dependent changes in the electronic absorption spectra of an aqueous reaction mixture, BNPP (1×10^{-4} M) and ZVI NPs (1×10^{-7} M). This process takes place at room temperature, and the final pH was 7.

In the Figure 3, the evolution in time of electronic absorption spectra for BNPP degradation by the interacting with the ZVI nanoparticles is displayed. The BNPP spectrum initially exhibits a single band at 289 nm, with an approximate 1.83 absorbance units. After 10 minutes of reaction a drastic change in the spectrum is observed. Two bands, the first is located at 239 nm, with 0.67 units and the second at 288 nm with 0.54 absorbance units are obtained. After 30 minutes and until one day of interaction of the BNPP with the ZVI NPs, the electronic absorption spectrum of reaction mixture remains without appreciable changes. This new spectrum were assigned to the formation of *p*-aminophenol (*p*-AP) and *p*-aminophenyl phosphate (*p*-APP), which are products that result from two consecutive processes; first occurs the hydrolysis of BNPP and subsequently happens reduction of the nitro group [18].

The mechanism proposed for the degradation of BNPP assisted by zero-valent iron NPs is shown in Scheme 1. Initially, the BNPP hydrolysis occurs through the P-O bonds breaking-off under action of the ZVI NPs. Thus, the molecule is divided into two parts forming the *p*-nitrophenol and *p*-nitrophenyl phosphate. Subsequently, due to the great reducing power of Fe nanoparticles, nitro groups are reduced to amines, in this case it is proposed that the water is the source of H+. The effectiveness of the reduction of nitroaromatic compounds by zero-valent iron gives as primary products aromatic amines, which is well documented in the literature [19-22]. Further, the mechanisms that have been published suggest that reduction of pollutant compounds in the presence of zero-valent iron occurs on the active sites of the surface of this metal [23].

Scheme 1. Suggested Mechanism of BNPP Degradation by interaction of this pollutant with the Fe^0 NPs surface to form *p*-aminophenol and *p*-aminophenyl phosphate.

In order to corroborate the second process of the proposed mechanism in the degradation of BNPP, *p*-NP and *p*-NPP were used as standards. These compounds were subjected to the same experimental conditions used in the degradation of BNPP and interacted with the Fe NPs. Firstly, the UV-visible spectra of *p*-NP and *p*-NPP versus time are recorded to determine their stability when they remains in aqueous solution.

Subsequently, the interaction of Fe NPs with *p*-NP was performed. In the Figure 4, the change of the electronic absorption spectrum of *p*-NP after 30 minutes of interaction with the iron particles is observed. After 1h, the spectra remained almost unchanged and were identified with the *p*-aminophenol spectrum. Also, the absorbance values are close to those of *p*-aminophenol (*p*-AP) prepared at the same concentration (1×10^{-4} M).

The Figure 5 shows the same process for monitoring by UV-vis spectroscopy in the interaction of the *p*-NPP with Fe^0 NPs. Again a drastic change occurs in the spectrum of this standard, evidencing a reaction by the reducing action of the Fe^0 NPs. In this case, it was not possible to compare it with the *p*-aminophenyl phosphate spectrum.
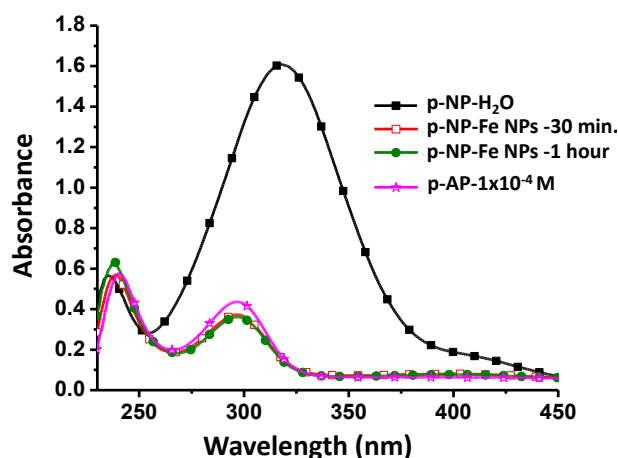
Figure 4. Time-dependent changes in the electronic absorption spectra of an aqueous reaction mixture, p- NP (1×10^{-4} M) and ZVI NPs (1×10^{-7} M), the final pH was 7.
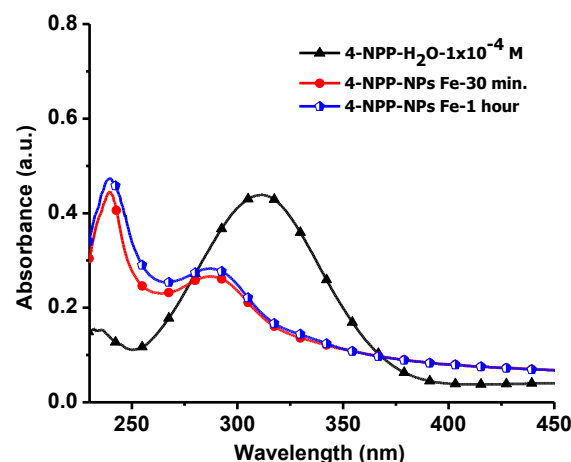

Figure 5. Time-dependent changes in the electronic absorption spectra of an aqueous reaction mixture, p- NPP (1×10^{-4} M) and ZVI NPs (1×10^{-7} M), the final pH was 7.

It is important to mention that the dispersion of the nanoparticles in water was also studied by UV-vis spectroscopy and no absorption bands corresponding to iron species were obtained. This result was corroborated with a new experiment, which is shown in Figure 6. The indicated figure exhibits the evolution in time of the electronic absorption spectra of BNPP solubilized in water. The water used to solubilize the BNPP previously for 30 minutes was in contact with the metallic Fe nanoparticles. The results of this experiment reveal that there are no Fe species soluble in the reaction medium that contribute significantly to the degradation of BNPP, at least under the reaction conditions in which the experiments were performed.
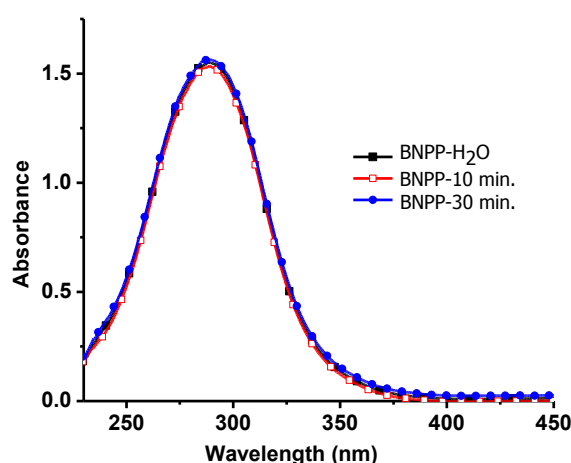

Figure 6. Electronic absorption spectra in time of an aqueous solution of BNPP (1×10^{-4} M). The water previously was in contact by 30 minutes with ZVI NPs under stirring. This process takes place at room temperature, and the final pH was 7.
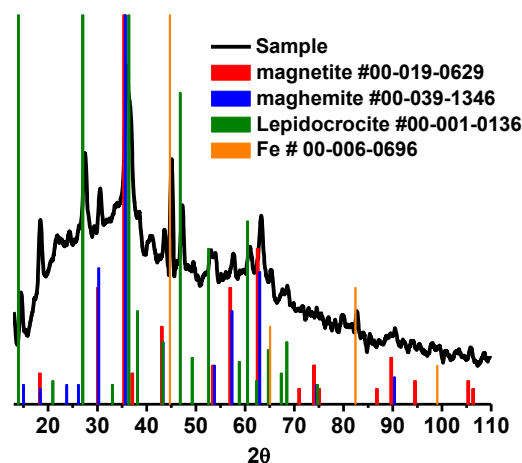

Figure 7. X-ray diffraction pattern of the isolated powder after the interaction between ZVI nanoparticles and BNPP in aqueous solution.

The degradation products of the Fe NPs was washed with water and acetone and characterized by X-Ray diffraction. The diffractogram obtained is represented in the Figure 7. It was detected

6

magnetite (Fe_3O_4) and/or maghemite (γ-Fe_2O_3) which have similar crystalline structure. Also, was identified lepidocrocite which is an oxohydroxo of iron (γ-FeOOH).

4. Concluding Remarks

Zerovalent iron nanoparticles with average diameter 10.2 ± 3.2 nm were synthesized by a reliable method. The ZVI nanocrystallines are able to degrade BNPP, under normal reaction conditions. The overall degradation process takes place in approximately 10 minutes. It was proposed a simple mechanism based in the reduction of organic contaminant compound of active sites on the surface of Fe^0 NPs. The by-products of BNPP are aromatic amines, which are more susceptible to biodegration than the original nitro compounds. The by-products of ZVI NPs were identified as magnetite (Fe_3O_4) and/or maghemite (γ-Fe_2O_3) and lepidocrocite which is an oxohydroxo of iron (γ-FeOOH).

5. References

[1] Westheimer F H, Why nature chose phosphates, 1987*, Science*, **235**, 1173.

[2] Bazzicalupi C, Benchini A, Berni E, Bianchi A, Fedi V, Fusi V, Giorgio C, Paoletti P and Valtancoli B, Carboxy and Diphosphate Ester Hydrolysis by a Dizinc Complex with a New Alcohol-Pendant Macrocycle, 1999*, Inorg. Chem*., **38**, 4115.

[3] Spiro T G and Stigliani W M, *Química Medioambiental*, segunda edición, **2004**, Pearson Educación.

[4] Jia-Qing X, Ci L., Min W, Bing-Ying J., Preparation of a new metallomicelle catalyst for the hydrolysis of bis(4-nitrophenyl) phosphate, 2013, *Chemical Papers,* **67(4)**, 365.

[5] Chin J, Banaszczyk M, Jubian V and Zou X, 1989, *J. Am. Chem. Soc.,* **111**, 186.

[6] Yuanqin Z, Fan L, Qingxiang X and Junru X, A study on the hydrolysis of bis(nitrophenyl)phosphate catalyzed by N-methyldiethanolamine-Ce(III) complex, 2004, *Int. J. Chem. Kinet.*, **36**(12), 687.

[7] Jiang W, Xu B, Lin Q, Li J, Liu F, Zeng X and Chen H, Metal-promoted hydrolysis of bis(*p*nitrophenyl) phosphate by trivalent manganese complexes with Schiff base ligands in Gemini micellar solution, 2008, *Colloid. Surf. A: Phys. Eng. Aspects*, **315**, 103.

[8] Kou D, Meng X-G, Liu Y, Du J, Kou X-M and Zeng X-C, Comparative studies on hydrolysis of bis(*p*nitrophenyl) phosphate catalyzed by short- and long-alkyl-multiamine metallomicelles, 2008, *Colloid. Surf. A:Physicochem. Eng. Aspects*, **324**, 189.

[9] Tafesse F and Eguzozie K, Efficient hydrolysis of 4-nitrophenylphosphate catalyzed by copper bipyridyl in microemulsions, 2009, *Ecotoxicol. Environ. Safety*, **72**, 954.

[10] Li F, Vipulanandan C and Mohanty K K, Microemulsion and solution approaches to nano-scale particle iron production for degradation of trichloroethylene, 2003, *Colloids Surf. A,* **223**, 103–112.

[11] Kim H, Hong H-J, Lee Y-J, Shin H-J, Yang J-W, Degradation of trichloroethylene by zero-valent iron immobilized in cationic exchange membrane, 2008, *Desalination*, **223**, 2 12.

[12] Nurmi J T, Tratnyek P G, Sarathy V, Baer D R, Amonette J E, Pecher K, Wang C, Linehan J C, Matson D W, Penn R L, Driessen M, Characterization and properties of metallic iron nanoparticles: Spectroscopy, electroscopy, electrochemistry and kinetics, 2005, *Environ. Sci. Technol.*, **39**, 1221.

[13] Li X-Q, Zhang W-X, Sequestration of metal cations with zerovalent iron nanoparticles, a study with high resolution X-ray photoelectron spectroscopy (HR-XPS), 2007, *J. Phys. Chem. C*, **111**, 6939.

[14] Poder S M, Darab J G, Bucher J, Caulder D, Craig I, Davis L, Edelstein N, Lukens W, Nitsche H, Rao L, Shuh D K, Mallouk T E, Surface Chemistry and Electrochemistry of Supported Zerovalent Iron Nanoparticles in the Remediation of Aqueous Metal Contaminants, 2001, *Chem. Mater.,* **13**, 479.

[15] Ma C, Wu Y, Dechlorination of perchloroetylene using zero-valent metal and microbial community, 2008, *Environ. Geol.,* **55**, 47.

[16] Shishido, T.; Morishima, R.; Yoshinaga, Y.; Hasegawa, S.; Tanaka, T., Effect of support on the suppression of hot spot formation in the partial oxidation of methane, 2009, *Chem. Lett.*, **38**(7), 720.

[17] Valle-Orta M, Diaz D, Vazquez-Olmos A R, Santiago P and Reguera E, Instantaneous synthesis of stable zerovalent metal nanoparticles under standard reaction conditions, 2008, *J.Phys. Chem. B*, **112**(46), 14427.

[18] Pradhan N, Pal A and Pal T, Catalytic reduction of aromatic nitro compounds by coinage metal nanoparticles, 2001, *Langmuir*, **17**(5), 1800.

[19] Agrawal A and Tratnyek P G, Reduction of nitroaromatic compounds by zero-valent iron metal, 1996 *Environ. Sci. Technol.*, **30**, 153.

[20] Devlin J F, Klausen J and Schwarzenbach R P, Kinetics of nitroaromatic reduction on granular iron in recirculating batch experiments, 1998*, Environ. Sci. Technol.*, **32**, 1941.

[21] Hayakawa K, Yoshimura T and Esumi K, Preparation of gold-dendrimer nanocomposites by laser irradiation and their catalytic reduction of 4-nitrophenol, 2003, *Langmuir*, **19**, 5517.

[22] Fleming I and Trost B M, Comprehensive organic synthesis. Vol. 8, 366, Pergamon Press, fifth impression, Elsevier, 2005.

[23] Weber E J, Iron-mediated reductive transformations: investigation of reaction mechanism, 1996, *Reser. Comm.*, **30**(2), 716.